Bi- and Trimetallic σ-Acetylide Complexes Connected through a Phenyl Ring in the Fe(Cp*)(dppe) Series

Tania Weyland,[†] Claude Lapinte,*[,†] Gilles Frapper,[‡] Maria José Calhorda,[§] Jean-François Halet,*[,‡] and Loic Toupet[∥]

Laboratoire de Chimie des Complexes de Métaux de Transition et Synthèse Organique, URA CNRS 415, Laboratoire de Chimie du Solide et Inorganique Moléculaire, URA CNRS 1495, and Laboratoire de Physique Cristalline, URA CNRS 804, Université de Rennes I, Campus de Beaulieu, 35042 Rennes Cedex, France, and Instituto de Tecnologia Quimica e Biologica, R. da Quinta Grande 6, 2780 Oeiras, Portugal

Received December 30, 1996[⊗]

Treatment of 1 equiv of the 1,3-bis(trimethylsilylethynyl)benzene with 2.3 equiv of [Fe(Cp*)(dppe)Cl] [**1**, Cp* = η^5-C_5Me_5, dppe = η^2-bis(diphenylphosphino)ethane], KF and KPF_6 salts in a methanol/THF mixture (10:1) produced the bis(iron) alkyne complex [{Fe(Cp*)(η^2-dppe)(C≡C−)}$_2$(1,3-C_6H_4)] (**2**) in 80% yield. Similarly, the trinuclear iron derivative [{Fe(Cp*)(η^2-dppe)(C≡C−)}$_3$(1,3,5-C_6H_3)] (**3**) was obtained from reaction of **1** with 1,3,5-tris(trimethylsilylethynyl)benzene (80% yield with respect to the organic ligand). The X-ray crystal structure of **3** shows that it crystallizes in the triclinic space group with unit-cell parameters of a = 18.142(6) Å, b = 18.652(8) Å, c = 20.108(6) Å, α = 113.72(3), β = 89.87(3), γ = 116.07(3)°, and Z = 2. The structure was solved and refined (6922 reflections) to the final values R = 0.081 and R_w = 0.069. Cyclic voltammetric analysis of complexes **2** and **3** from −1.0 to +0.5 V displays two and three one-electron reversible oxidation waves, respectively. The redox processes are all separated by 0.130 ± 0.010 V, indicating significant electronic communication between the metal centers. A theoretical treatment using density functional molecular orbital calculations has been made on compounds **2**, **3**, and the related compound [{Fe(Cp*)(η^2-dppe)(C≡C−)}$_2$(1,4-C_6H_4)]. These results verify the experimental structure of **3** and allow an interpretation of its electronic structure.

Conjugated organic molecules have been the subject of intensive studies because of their interesting properties and potential applications to advanced materials.[1−6] More recently, in an effort to exploit electronic- and photonic-based cooperation between individual transition metal subunits of a molecular assembly having a delocalized π-backbone, new organometallic complexes have emerged as a promising class of molecules for future use in the areas of nonlinear optics and molecular electronics.[7−9] Specific properties of transition metal containing molecules result primarily from the ability of the metal to participate in π-delocalization, as well as the potential for interaction of the transition metal d-orbitals with the conjugated π-orbitals of the organic moiety.[10−14] Moreover, the metal-to-ligand and ligand-to-metal charge transfers, which constitute one of the properties of the organometallic complexes, produce significant reordering of the π-electron distribution of the ligands coordinated to the metal centers.[15,16]

Recent works on linear and conjugated C2 to C20-bridged bimetallic systems have demonstrated that σ-acetylide ligands constitute the most efficient link between organometallic building blocks.[17−22] Metal acetylide complexes with a large extent of π-delocalization have afforded numerous bimetallic and polymetallic complexes linked by conjugated and rigid −C≡C−aryl−C≡C− backbones with a variety of metals including *inter alia*, Co,[23,24] Fe,[25−28] Ru,[29−31] Mn,[32] Ni, Pd, Pt,[33,34] Rh,[35−37] and Ir.[38]

Besides our efforts devoted to the synthesis of an elemental carbon chain bridging two iron centers (**I**) and the study of the special coupling properties of the $-C_x$

[†] Laboratoire de Chimie des Complexes de Métaux de Transition et Synthèse Organique.
[‡] Laboratoire de Chimie du Solide et Inorganique Moléculaire.
[§] Instituto de Tecnologia Quimica e Biologica.
[∥] Laboratoire de Physique Cristalline.
[⊗] Abstract published in *Advance ACS Abstracts,* April 1, 1997.

(1) Iwamura, H. *Adv. Phys. Org. Chem.* **1990**, *26*, 179.
(2) Dougherty, D. A. *Acc. Chem. Res.* **1991**, *24*, 88−94.
(3) Iwamura, H.; Koga, N. *Acc. Chem. Res.* **1993**, *26*, 346−351.
(4) Rajca, A. *Chem. Rev.* **1994**, *94*, 871−893.
(5) Miller, J. S.; Epstein, A. J. *Angew. Chem., Int. Ed. Engl.* **1994**, *33*, 385−415.
(6) Yoshizawa, K.; Hoffmann, R. *Chem. Eur. J.* **1995**, *1*, 403.
(7) Beck, W.; Niemer, B.; Wieser, M. *Angew. Chem., Int. Ed. Engl.* **1993**, *32*, 923−949.
(8) Hunter, A. D. *Organometallics* **1989**, *8*, 1118−1120.
(9) Chukwu, R.; Hunter, A. D.; Santarsiero, B. D. *Organometallics* **1992**, *11*, 589−597.
(10) Pollagi, T. P.; Stoner, T. C.; Dallinger, R. F.; Gilbert, T. M.; Hopkins, M. D. *J. Am. Chem. Soc.* **1991**, *113*, 703−704.
(11) Calabrese, J. C.; Cheng, L.-T.; Green, J. C.; Marder, S. R.; Tam, W. *J. Am. Chem. Soc.* **1991**, *113*, 7227−7232.
(12) Meyers, L. K.; Langhoff, C.; Thompson, M. E. *J. Am. Chem. Soc.* **1992**, *114*, 7560−7561.
(13) Lichtenberger, D. L.; Renshaw, S. K.; Bullock, R. M. *J. Am. Chem. Soc.* **1993**, *115*, 3276−3285.
(14) Lichtenberger, D. L.; Renshaw, S. K.; Wong, A.; Tagge, C. D. *Organometallics* **1993**, *12*, 3522−3526.
(15) Frasier, C. C.; Guha, S.; Chen, W. P.; Cockerham, M. P.; Porter, P. L.; Chauchard, E. A.; Lee, C. H. *Polymer* **1987**, *28*, 553−555.
(16) Stoner, T. C.; Dallinger, R. F.; Hopkins, M. D. *J. Am. Chem. Soc.* **1990**, *112*, 5651−5653.
(17) Le Narvor, N.; Lapinte, C. *J. Chem. Soc., Chem. Commun.* **1993**, 357−359.
(18) Zhou, Y.; Seyler, J. W.; Weng, W.; Arif, A. M.; Gladysz, J. A. *J. Am. Chem. Soc.* **1993**, *115*, 8509−8510.
(19) Seyler, J.; Weng, W.; Zhou, Y.; Gladysz, J. A. *Organometallics* **1993**, *12*, 3802−3804.
(20) Bartik, T.; Bartik, B.; Brady, M.; Dembinski, R.; Gladysz, J. A. *Angew. Chem., Int. Ed. Engl.* **1996**, *35*, 414−417.
(21) Wong, A.; Kang, P. C. W.; Tagge, C. D.; Leon, D. R. *Organometallics* **1990**, *9*, 1992−1994.
(22) Crescenzi, R.; Sterzo, C. L. *Organometallics* **1992**, *11*, 4301−4305.

S0276-7333(96)01102-8 CCC: $14.00

Scheme 1

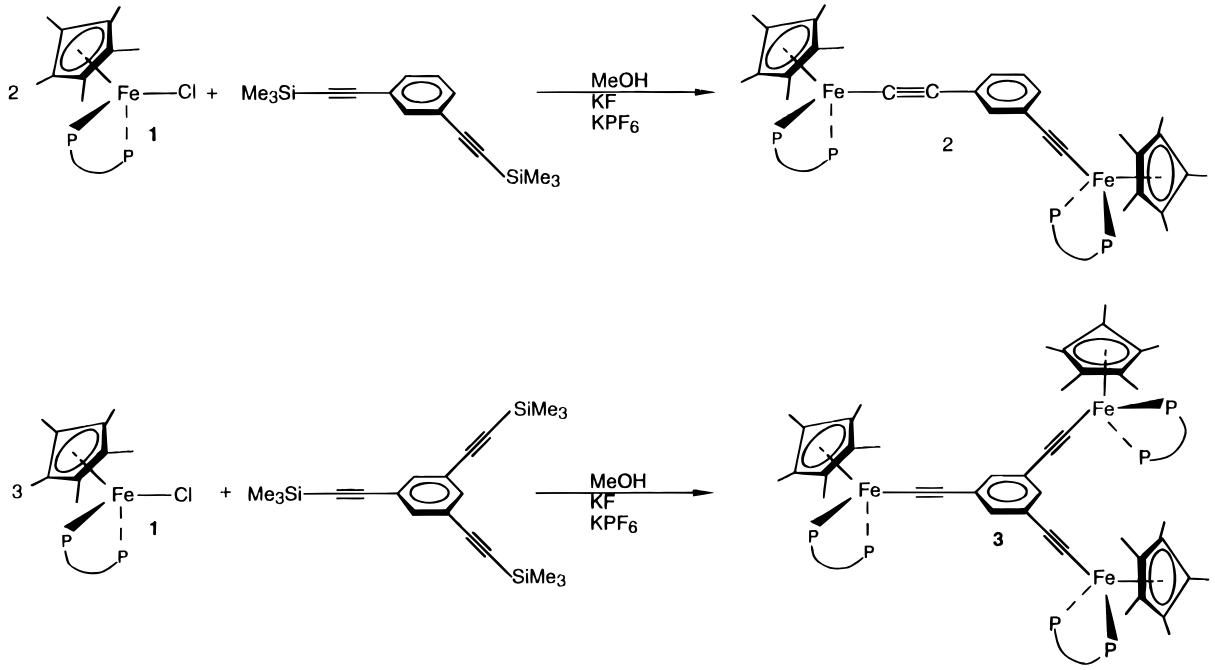

carbon chain, we are also involved in the construction of molecular assemblies containing several organometallic building blocks covalently connected through an all-π-delocalized organic spacer with a precisely controlled geometry.[28] The study of the mutual influence

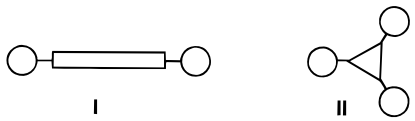

between the metal centers of a two-dimensional molecule in which three electron-rich organometallic building blocks are spanned with a poly(ethynyl)aryl ligand (**II**) was the aim of this work. For this purpose, we have used the 1,3,5-tris(trimethylsilylethynyl)benzene ligand to connect three electron-rich organoiron units Cp*Fe(dppe). We report here (i) the synthesis of the trinuclear complex [{Fe(Cp*)(η^2-dppe)(C≡C−)}$_3$(1,3,5-C$_6$H$_3$)] (**3**), (ii) its characterization, including an X-ray crystal structure, (iii) a cyclic voltammetry study, which reveals metal−metal electronic communication, and (iv) its electronic structure obtained with density functional calculations. The synthesis and the comparative study of the bimetallic complex [{Fe(Cp*)(η^2-dppe)(C≡C−)}$_2$-(1,3-C$_6$H$_4$)] (**2**) was also carried out as a complementary investigation.

Results and Discussion

Synthesis of the Polynuclear Complexes [{Fe(Cp*)(η^2-dppe)(C≡C)−}$_2$ (1,3-C$_6$H$_4$)] (2) and [{Fe(Cp*)(η^2-dppe)(C≡C−)}$_3$(1,3,5-C$_6$H$_3$)] (3). Complex **2** was prepared from the iron halide Fe(η^5-C$_5$Me$_5$)(η^2-dppe)Cl (**1**)[39] and 1,3-bis(trimethylsilylethynyl)benzene.[40−45] Treatment of 1 equiv of the bis(trimethylsilylalkyne) with 2.3 equiv of the chloro complex **1** in a methanol/THF mixture (10:1) in the presence of KF and KPF$_6$ salts produced, after refluxing 16 h, an orange solution. The bis(iron) alkyne complex [{Fe(Cp*)(η^2-dppe)(C≡C−)}$_2$(1,3-C$_6$H$_4$)] (**2**) was isolated from this solution as an orange powder in 80% yield (Scheme 1). In this one-step procedure, the 1,3-bis(ethynyl)benzene bridging ligand is generated in situ by the fluoride-induced cleavage of the terminal trimethylsilyl groups (eq 1).

$$\mathrm{Ar{-}(C{\equiv}C{-}SiMe_3)_2 + 2KF \xrightarrow{MeOH} Ar{-}(C{\equiv}C{-}H)_2 + 2Me_3Si{-}F + 2MeOK} \quad (1)$$

$$\mathrm{2[Fe(Cp^*)(dppe)Cl] + 2KPF_6 \rightarrow 2[Fe(Cp^*)(dppe)][PF_6] + 2KCl} \quad (2)$$

As extensively described, the PF_6^- anion acts as a halide abstractor[46] (eq 2) to promote the complexation of the terminal alkyne at the iron center, giving the vinylidene complex isolated in many cases as the final

(23) Khan, M. S.; Pasha, N. A.; Kakkar, A. K.; Raithby, P. R.; Lewis, J.; Buhrmann, K.; George, A. V.; Lashi, F.; Malouf, E. V.; Zamello, P. J. *J. Organomet. Chem.* **1992**, *435*, 347−356.
(24) Johnson, B. F. G.; Kakkar, A. K.; Khan, M. S.; Lewis, J. *J. Organomet. Chem.* **1991**, *401*, C43−C45.
(25) Field, L. D.; George, A. V.; Laschi, F.; Malouf, E. V.; Zamello, P. J. *J. Organomet. Chem.* **1992**, *435*, 347−356.
(26) Johnson, B. F. G.; Kakkar, A. K.; Khan, M. S. *J. Organomet. Chem.* **1991**, *409*, C12−C14.
(27) Hunter, A. D.; Szigety, A. B. *Organometallics* **1989**, *8*, 2670−2679.
(28) Le Narvor, N.; Lapinte, C. *Organometallics* **1995**, *14*, 634−639.
(29) Lavastre, O.; Even, M.; Dixneuf, P. H.; Pacreau, A.; Vairon, J. P. *Organometallics* **1996**, *15*, 1530−1531.
(30) Atherton, Z.; Faulkner, C. W.; Ingham, S. L.; Kakkar, A. K.; Khan, M. S.; Lewis, J.; Nicholas, J. L.; Raithby, P. R. *J. Organomet. Chem.* **1993**, *462*, 265−270.
(31) Davies, S. J.; Johnson, B. F. G.; Lewis, J.; Raithby, P. R. *J. Organomet. Chem.* **1991**, *414*, C51−C53.
(32) Davies, S. J.; Johnson, B. F. G.; Lewis, J.; Khan, M. S. *J. Organomet. Chem.* **1991**, *401*, C43−C45.
(33) Khan, M. S.; Davies, S. J.; Kakkar, A. K.; Schwartz, D.; Lin, B.; Johnson, B. F. G.; Lewis, J. *J. Organomet. Chem.* **1992**, *424*, 87−97.
(34) Takahashi, S.; Morimoto, H.; Murata, E.; Kataoka, S.; Sonogashira, K.; Hagihara, N. *J. Polym. Sci., Polym. Chem. Ed.* **1982**, *20*, 565−573.
(35) Rappert, T.; Nürnberg, O.; Werner, H. *Organometallics* **1993**, *12*, 1359−1364.
(36) Davies, S. J.; Johnson, B. F. G.; Kahn, M. S.; Lewis, J. *J. Chem. Soc., Chem. Commun.* **1991**, 187−188.
(37) Fyfe, H. B.; Mlekuz, M.; Zargarian, D.; Taylor, N. J.; Marder, T. B. *J. Chem. Soc., Chem. Commun.* **1991**, 188−189.
(38) Tykwinski, R. R.; Stang, P. J. *Organometallics* **1994**, *13*, 3203−3208.

product of the reaction (eq 3). However, in our conditions, the cleavage of the trimethylsilyl group is associated with the formation of a stoichiometric amount of a strong base. This base, in situ, deprotonates the vinylidene intermediate, allowing the formation of the bis(iron alkynyl) complex **2** as the final product of the reaction (eq 4). It is noteworthy that the use of the bis(trimethylsilylethynyl)benzene as the starting material is particularly convenient, since the direct formation of complex **2** could not be obtained working with the terminal ethynyl derivative and a base. Indeed, the reaction between an alkyne and the iron complex **1** in the presence of a stoichiometric amount of potassium methylate or *tert*-butylate provides the iron hydride Fe(η^5-C_5Me_5)(η^2-dppe)H. In the experimental conditions, it was shown that the 16-electron species [Fe(η^5-C_5Me_5)(η^2-dppe)][PF_6], in equilibrium with the chloro complex **1**, is easily reduced by a strong base into the 17-electron iron(I) radical [Fe(η^5-C_5Me_5)(η^2-dppe)]$^\bullet$. This very reactive species abstracts a hydrogen atom from the solvent to produce the iron hydride.[47]

$$2[Fe(Cp^*)(dppe)][PF_6] + Ar{-}(C{\equiv}C{-}H)_2 \rightarrow [\{Fe(Cp^*)(dppe)(=C{=}CH)\}_2{-}Ar][PF_6]_2 \quad (3)$$

$$[\{Fe(Cp^*)(dppe)(=C{=}CH)\}_2{-}Ar][PF_6]_2 + 2MeOK \rightarrow [\{Fe(Cp^*)(dppe)(C{\equiv}C)\}_2{-}Ar] + 2MeOH + 2KPF_6 \quad (4)$$

2

Poly(ethynyl)benzene derivatives having more than two ethynyl groups were described as potentially explosive compounds.[45,48] Therefore, our procedure is interesting in opening a safe route to compounds with a nuclearity higher than two. Thus, treatment of 1 equiv of 1,3,5-tris(trimethylsilylethynyl)benzene[40,44] with 3.2 equiv of the chloro complex **1** in the same conditions produced after 60 h an orange solution, from which the trinuclear iron derivative [{Fe(Cp^*)(η^2-dppe)($C{\equiv}C-$)}$_3$-(1,3,5-C_6H_3)] (**3**) was isolated as a light-orange solid in 80% yield, with respect to the organic bridging building block (Scheme 1). The reaction is significantly slower than that of the bis(trimethylsilylethynyl)benzene. On the other hand, working with an excess of the iron chloro complex allowed isolation of the trinuclear compound free of any mono- or binuclear impurities.

The analytically pure complexes **2** and **3** were characterized by IR and multinuclear NMR spectroscopies. Specifically, the IR spectra show a typical absorption for the carbon−carbon triple bond at 2051 ± 1 cm^{-1} for the bimetallic and trimetallic complexes **2** and **3**, as well as for the previously reported mononuclear species [Fe(Cp^*)(dppe)($C{\equiv}C{-}C_6H_5$)] (**4**).[49] The $\nu_{(C\equiv C)}$ for [Fe(Cp^*)(dppe)($C{\equiv}C{-}t$-Bu)] was also observed at a very close position (2066 cm^{-1}).[49] Similarly, the $\nu_{(C\equiv C)}$ frequency in the [Fe(Cp)$(CO)_2$($C{\equiv}CR$)] series is also weakly sensitive to the electronic properties of the R group born by the acetylide ligand.[13]

The similar $\nu_{(C\equiv C)}$ frequencies observed for a series of metal−acetylide complexes could be due to the cancellation of two effects:an increase of $\nu_{(C\equiv C)}$ that occurs because of the substitution of the phenyl ring by a more electron donating fragment (i.e., *tert*-butyl group) and a decrease of the $\nu_{(C\equiv C)}$ frequency due to a weaker effect of the π*-back-bonding from the metal into the carbon−carbon π* orbital.[50] The weaker $\nu_{(C\equiv C)}$ frequency of ca. 55 cm^{-1} observed in the more electron-rich Cp^*Fe(dppe) series than in the $CpFe(CO)_2$ series also suggests that π*-back-bonding could take place. However, it was shown from photoelectron spectroscopy studies of the metal−acetylide interactions that back-bonding is extremely small compared to the metal dπ-acetylide−π interactions.[13] A significant metal-to-metal electronic communication is expected in the polynuclear complexes **2** and **3**, if an extensive mixing occurs between the metal dπ-orbitals, the C≡C π-orbitals, and the phenyl ring orbitals.

The ^{13}C resonances of the ethynyl fragments were not observed in the ^{13}C NMR spectra of the complexes **2** and **3** due to their poor solubility. The ^{31}P NMR spectrum (CD_2Cl_2, 20 °C) of binuclear compound **2** exhibits a sharp resonance at δ 89.37, whereas the spectrum of the compound **3** consists of a broad signal at δ 101.3 (20 °C, C_7D_8). The line broadening of the ^{31}P NMR signal, diagnostic of steric hindrance in the trinuclear complex, reveals slow rotation processes on the NMR time scale. Upon warming to 90 °C, the signal continues to broaden and coalescence is reached at 90 °C. In contrast, the signal sharpens progressively as the temperature decreases but a single resonance is still observed at −80 °C (see Supporting Information). This surprising behavior could be the result of the different orientation of the organoiron building blocks with respect to the plane of the bridging arene. Consequently, two dppe ligands could be located on one side of this plane and the third one on the other side, rendering the two faces of the molecule magnetically nonequivalent.

X-ray Crystal Structure of [{Fe(Cp^*)(η^2-dppe)($C{\equiv}C-$)}$_3$(1,3,5-C_6H_3)] (3). To provide insight into the mutual arrangement of the organometallic building blocks and their steric interactions, an X-ray crystal analysis of **3** was determined. Single crystals were grown by slow diffusion of pentane into a CH_2Cl_2 solution of **3**. The unit cell contains two molecules. The molecular structure of the trinuclear complex **3** is shown in Figure 1. The X-ray data conditions are summarized in Table 1. Selected bond distances and bond angles are collected in Table 2.

Complex **3** crystallizes in the triclinic space group $P\bar{1}$ with a molecule of pentane. As usually observed for many piano-stool complexes, the three organoiron centers adopt a pseudooctahedral geometry. Three coor-

(39) Roger, C.; Hamon, P.; Toupet, L.; Rabaâ, H.; Saillard., J.-Y.; Hamon, J.-R.; Lapinte, C. *Organometallics* **1991**, *10*, 1045−1054.
(40) Berris, B. C.; Hovakeemian, G. H.; Lai, Y.-H.; Vollhardt, K. P. C. *J. Am. Chem. Soc.* **1986**, *107*, 5670−5687.
(41) Diercks, R.; Vollhardt, K. P. C. *Angew. Chem., Int. Ed. Engl.* **1986**, *25*, 266−268.
(42) Diercks, R.; Armstrong, J. C.; Boese, R.; Vollhardt, K. P. C. *Angew. Chem., Int. Ed. Engl.* **1986**, *25*, 268−269.
(43) Blanco, L.; Helson, H. E.; Hirthammer, M.; Mestdagh, H.; Spyroudis, S.; Vollhardt, K. P. C. *Angew. Chem., Int. Ed. Engl.* **1987**, *26*, 1246−1247.
(44) Boese, R.; Green, J. R.; Mittendorf, J.; Mohler, D. L.; Vollhardt, K. P. C. *Angew. Chem., Int. Ed. Engl.* **1992**, *12*, 1643−1645.
(45) Neenan, T. X.; Whitesides, G. M. *J. Org. Chem.* **1988**, *55*, 2489−2496.
(46) Bruce, M. I. *Chem. Rev.* **1991**, *91*, 197−257.
(47) Hamon, P.; Toupet, L.; Hamon, J.-R.; Lapinte, C. *Organometallics* **1996**, *15*, 10−12.
(48) Rutledge, T. F. Acetylenic Compounds. Preparation and Substitution; Reinhold Book Corporation: New York, 1968.
(49) Connelly, N. G.; Gamasa, M. P.; Gimeno, J.; Lapinte, C.; Lastra, E.; Maher, J. P.; Narvor, N. L.; Rieger, A. L.; Rieger, P. H. *J. Chem. Soc., Dalton Trans.* **1993**, 2575−2578.
(50) Kostic, N. M.; Fenske, R. F. *Organometallics* **1982**, *1*, 974−982.

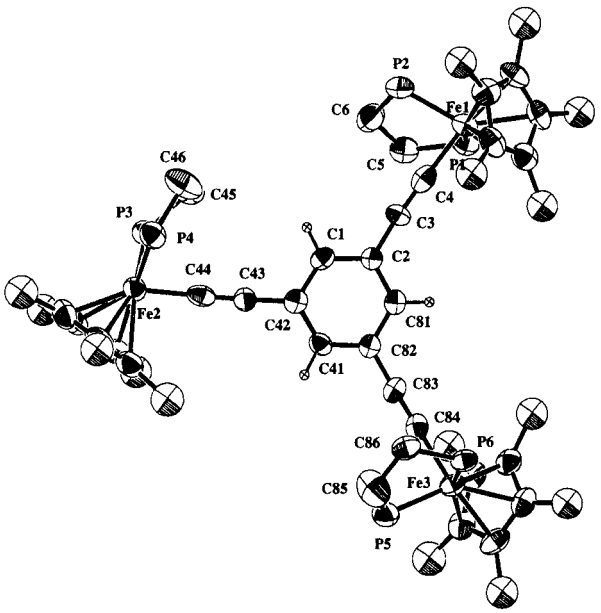

Figure 1. X-ray structure of the complex [FeCp*(η^2-dppe)(C≡C)]$_3$(μ-1,3,5-C$_6$H$_3$) (view perpendicular to the plane of the central phenyl ring). The phenyl groups of the dppe ligands have been omitted for clarity.

Table 1. Experimental Crystallographic Data for 3[a]

formula	$C_{120}H_{120}Fe_3P_6 \cdot C_5H_{12}$
fw	1987.83
cryst syst	triclinic
space group	$P\bar{1}$
a, Å	18.142(6)
b, Å	18.652(8)
c, Å	20.108(6)
α, deg	113.72(3)
β, deg	89.87(3)
γ, deg	116.07(3)
V, Å^3	5468(4)
Z	2
D_{calcd}, g/cm^3	1.207
F(000)	2100
μ(Mo Kα), cm^{-1}	5.25
T, K	294
cryst size, mm	0.30 × 0.30 × 0.45
max 2*θ*, deg	50
scan type	$\omega/2\theta = 1$
t_{max}/measure, s	60
variance of standards	0.3%
range of *hkl*	0, 21; −22, +22; −23, +23
no. of reflns measd	19799
no. of reflns obsd ($I > \sigma(I)$)	6922 (4σ)
R	0.081
R_w	0.069
S_w	3.96
residual density e Å^{-3}, Δ/σ	0.22, 0.33

[a] $w = 1/\sigma(F_o)^2 = [\sigma^2(I) + (0.04F_o^2)^2]^{-1/2}$.

dination positions are occupied by the Cp* ring, whereas the two phosphorus atoms and the Cα carbon of the ethynyl fragments are positioned at the three remaining sites. The bond distances and bond angles of the Cp*Fe(dppe) units are essentially identical and compare well with the data determined for related mononuclear compounds. The Fe−C and C≡C bond lengths (Table 3) are close to those reported for the related complexes CpFe(CO)$_2$(C≡CPh),[51] Cp*Fe(CO)$_2$(C≡CPh), and Cp*Fe(CO)$_2$(C≡CH).[52] Only a weak contraction of the Fe−C bond lengths (0.02 Å) associated with a concommitant and slight lengthening of the acetylide C≡C bond (0.03 Å) is noted in compound **3**. The bridging phenyl ring is essentially planar, and the deviation from coplanarity of the tris(ethynyl)benzene spacer is only small (average 0.037 Å). The three iron atoms are positioned above and below the plane containing the connecting arene with a deviation of 0.28, −0.21, and −0.32 Å.

The three planes defined by the α carbon atoms of the ethynyl ligands, the iron atoms, and the centroids of the Cp* rings are tilted relative to the plane of the central phenyl with angles of 5.07°, 60.02°, and 241.74°. Such orientations must be the result of a compromise between the sterically favored disposition of the Cp* and bulky dppe ligands and electronic factors. The electronically favored orthogonal or perpendicular orientation of the planes of the Cp* ligands with respect of the plane of the tris(ethynyl)benzene would maximize conjugation but yield unacceptably short distances. The three metal centers are located at the vertices of an almost equilateral triangle, with intramolecular distances of 10.05, 10.32, and 10.48 Å. These distances are significantly longer than the iron−iron intermolecular distances of 9.14, 9.58, and 10.05 Å. The three

Table 2. Selected Bond Distances (Å) and Angles (deg) for 3

Fe(1)−P(1)	2.178(3)	C(83)−C(84)	1.21(1)
Fe(1)−P(2)	2.166(3)	C(84)−C(83)	1.21(1)
Fe(2)−P(3)	2.161(3)	C(3)−C(2)	1.42(1)
Fe(2)−P(4)	2.168(3)	C(42)−C(43)	1.42(2)
Fe(3)−P(5)	2.181(4)	C(82)−C(83)	1.41(1)
Fe(3)−P(6)	2.170(3)	C(1)−C(2)	1.38(2)
Fe(1)−Cp*$_{(centroid\ 1)}$	1.750	C(2)−C(81)	1.39(1)
Fe(2)−Cp*$_{(centroid\ 2)}$	1.742	C(81)−C(82)	1.41(1)
Fe(3)−Cp*$_{(centroid\ 3)}$	1.738	C(41)−C(82)	1.38(2)
Fe(1)−C(4)	1.90(1)	C(41)−C(42)	1.39(1)
Fe(2)−C(44)	1.89(1)	C(1)−C(42)	1.41(1)
Fe(3)−C(84)	1.92(1)	Fe(1)−Fe(2)	10.05
C(4)−C(3)	1.24(2)	Fe(2)−Fe(3)	10.48
C(44)−C(43)	1.23(2)	Fe(1)−Fe(3)	10.32

P(1)−Fe(1)−P(2)	84.7(1)	P(6)−Fe(3)−C(84)	83.7(4)
P(3)−Fe(2)−P(4)	85.7(1)	Fe(1)−C(4)−C(3)	178(1)
P(5)−Fe(3)−P(6)	85.9(1)	Fe(2)−C(44)−C(43)	177.4(9)
P(1)−Fe(1)−C(4)	84.8(3)	Fe(3)−C(84)−C(83)	178.4(8)
P(2)−Fe(1)−C(4)	83.8(3)	C(4)−C(3)−C(2)	173(1)
P(3)−Fe(2)−C(44)	83.7(2)	C(4)−C(43)−C(42)	177.(1)
P(4)−Fe(12)−C(44)	83.5(3)	C(84)−C(83)−C(82)	1175.5(9)
P(5)−Fe(3)−C(84)	84.1(4)		

Cp*$_{(centroid)}$−Fe(1)−C(4)/planar tris(ethynylbenzene)	36.1
Cp*$_{(centroid)}$−Fe(2)−C(4)/planar tris(ethynylbenzene)	5.1
Cp*$_{(centroid)}$−Fe(3)−C(4)/planar tris(ethynylbenzene)	298.3

Table 3. Electrochemical Data for Compounds 2 and 3, in CH_2Cl_2 (0.1 M [*n*Bu$_4$N][PF$_6$]; 20 °C, Pt Electrodes, Sweep Rate 0.100 V s^{-1})[a]

complexes	E_{p_c} (V)	E_{p_a} (V)	ΔE_p (V)	E_0 (V)	ΔE_0 (V)	K_c
2	−0.140	−0.060	0.080	−0.100		
	−0.270	−0.180	0.090	−0.225	0.130	1.3×10^2
3	−0.291	−0.219	0.073	−0.255	0.130	1.3×10^2
	−0.159	−0.091	0.068	−0.125	0.130	1.3×10^2
	−0.030	0.032	0.062	0.000		
4	−0.350	−0.280	0.070	−0.315	0.260	2.55×10^4
	−0.090	−0.020	0.070	−0.055		

[a] Potentials are given in V vs SCE; the ferrocene-ferrocenium couple (0.460 V vs SCE) was used as an internal calibrant for the potential measurements.

(51) Goddard, R.; Howard, J.; Woodward, P. J. *J. Chem. Soc., Dalton Trans.* **1974**, 2025−2027.

(52) Akita, M.; Terada, M.; Oyama, S.; Moro-Oka, Y. *Organometallics* **1990**, *9*, 816−825.

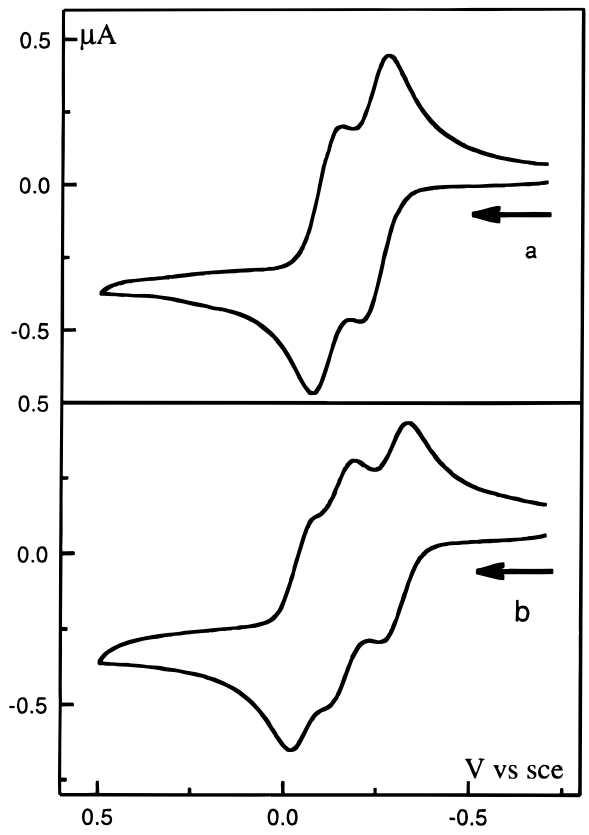

Figure 2. Cyclic voltammograms for (a) [FeCp*(η^2-dppe)(C≡C)]$_2$(μ-1,3-C_6H_4) (**2**) and (b) [FeCp*(η^2-dppe)-(C≡C)]$_3$(μ-1,3,5-C_6H_3) (**3**) in 0.1 M [nBu_4N][PF_6]/CH_2Cl_2 (Pt electrode; V vs SCE; scan rate 100 mV/s; 20 °C).

equivalent iron building blocks are crystallographically nonequivalent, owing to their different orientations. Furthermore, the associated intra- and intermolecular nanoscale metal−metal distances constitute the major interest of this molecule. Cyclic voltamograms were recorded to address the question of the mutual interaction between the metal centers.

Cyclic Voltammetric Analysis of [{Fe(Cp*)(η^2-dppe)(C≡C−)}$_2$(1,3-C_6H_4)] (2) and [{Fe(Cp*)(η^2-dppe)(C≡C−)}$_3$(1,3,5-C_6H_3)] (3). The initial scan in the cyclic voltamogram of complex **2** from +0.5 to −1.0 V (vs standard calomel electrode (SCE)) is characterized by two reversible waves in dichloromethane with the i_{p_a}/i_{p_c} current ratio of unity and a wave separation (ΔE_0) of 0.130 V (Figure 2). This means that at the platinum electrode the neutral dimer undergoes two successive one-electron oxidations to yield the mono- and the dications, respectively (eq 5).

$$\underset{\mathbf{2}}{\text{Fe(II)−Fe(II)}} \overset{-e}{\rightleftharpoons} \underset{\mathbf{2^+}}{\text{[Fe(II)−Fe(III)]}^+} \overset{-e}{\rightleftharpoons} \underset{\mathbf{2^{2+}}}{\text{[Fe(III)−Fe(III)]}^{2+}} \quad (5)$$

As shown in Table 3, the anodic and cathodic peak separation ($|E_{p_a} - E_{p_c}|$) for the two redox systems is close to 0.060 V with a 0.100 V s^{-1} sweep rate. Similarly, the cyclic voltamogram of the trinuclear complex **3** displays three reversible waves, with a current ratio of unity, and a peak to peak separation close to 0.060 V. Comparison of the oxidation potentials of the trinuclear compound **3** with those of dimer **2** and the mononuclear complex **4** reveals the trend expected for weakly coupled mixed-valence systems.[53] Thus, the first oxidation potentials corresponding to the redox system Fe(II)Fe-(II)Fe(II)/Fe(II)Fe(II)Fe(III) is observed 0.04 V below that of the Fe(II)Fe(II)/Fe(II)Fe(III) system observed for the dimer **2** and 0.06 V below that of the Fe(II)/Fe(III) system previously reported for the mononuclear derivative **4**. Note that the same wave separation was found between the three redox systems ($|\Delta E_0| = 0.130 \pm 0.010$ V) of the three-metal-center compound, exactly the same that those measured for the bimetallic complex **2**.

The comproportionation constant K_c relative to the equilibria in eqs 6−8 can be calculated from the wave splitting for compounds **2** and **3** (Table 3).

$$\underset{\mathbf{2}}{\text{Fe(II)−Fe(II)}} + \underset{\mathbf{2^{2+}}}{\text{[Fe(III)−Fe(III)]}^{2+}} \rightleftharpoons 2\underset{\mathbf{2^+}}{\text{[Fe(II)−Fe(III)]}^+} \quad (6)$$

$$\underset{\mathbf{3}}{\text{Fe(II)−Fe(II)−Fe(II)}} + \underset{\mathbf{3^{2+}}}{\text{[Fe(II)−Fe(III)−Fe(III)]}^{2+}} \rightleftharpoons 2\underset{\mathbf{3^+}}{\text{[Fe(II)−Fe(II)−Fe(III)]}^+} \quad (7)$$

$$\underset{\mathbf{3^+}}{\text{[Fe(II)−Fe(II)−Fe(III)]}^+} + \underset{\mathbf{3^{3+}}}{\text{[Fe(III)−Fe(III)−Fe(III)]}^{3+}} \rightleftharpoons 2\underset{\mathbf{3^{2+}}}{\text{[Fe(II)−Fe(III)−Fe(III)]}^{2+}} \quad (8)$$

These values indicate that the mixed-valence species are stable enough to predominate in solution. Moreover, the mixed-valence compounds $\mathbf{3}^+$ and $\mathbf{3}^{2+}$ for which one and two odd electrons are delocalized on three metal centers, respectively, are expected to have very similar stabilities.

The dependence of K_c on the metal−metal distance has been discussed on the basis of electrostatic interaction between the added charges.[54] Since this factor constitutes the dominant effect on K_c, a comparison must be made between compounds having a similar metal−metal separation. Thus, in the widely investigated series of biferrocenylpolyenes and biferrocenylenes, both the metal−metal distances and the redox potentials are known for a large number of complexes.[55−57] Similarly, for diferrocenylbutadiyne and the diferrocenylbutadiene, the metal−metal distance was estimated to be close to 9.2 Å, assuming a trans geometry of the ferrocenyl units. The wave splitting between the Fe(II)−Fe(II)/Fe(II)−Fe(III) and Fe(II)−Fe-(III)/Fe(III)−Fe(III) redox systems was reported to be 0.100 and 0.130 V, respectively.[58] In our system, similar K_c values were observed for an iron−iron distance that was longer. This is noteworthy since it was recently reported that diferrocenylpolyenes are the best systems, so far, to study long distance intervalence electron transfer.[58] Consequently, the two-dimensional bis- or tris(ethynyl)benzene organic moiety acts as a connector between the organoiron building blocks to convey sig-

(53) Creutz, C. *Prog. Inorg. Chem*. **1983**, *30*, 1−73.
(54) Reimers, J. R.; Hush, N. *Inorg. Chem*. **1990**, *29*, 3686−3697.
(55) Le Vanda, C.; Cowan, D. O.; Leitch, C.; Bechgaard, K. *J. Am. Chem. Soc.* **1974**, *96*, 6788−6789.
(56) Le Vanda, C.; Bechgaard, K.; Cowan, D. O. *J. Org. Chem*. **1976**, *41*, 2700−2704.
(57) Sutton, J. E.; Taube, H. *Inorg. Chem*. **1981**, *20*, 3125−3134.
(58) Ribou, A.-C.; Launay, J.-P.; Sachtleben, M. L.; Li, H.; Spangler, C. W. *Inorg. Chem*. **1996**, *35*, 3735−3740.

Table 4. Optimized Bond Distances (Å) for Models 2-H, 3-H, and 4-H

	4-H	**2**-H	**3**-H	**3**[a]
Fe−C(α)	1.882	1.879	1.893	1.90
C(α)−C(β)	1.236	1.235	1.238	1.23
C(β)−C(1)	1.423	1.423	1.430	1.42
C(1)−C(2)[b]	1.405	1.405	1.409	1.39

[a] Experimental bond distances (averaged). [b] C−C distance in the phenyl ring.

nificant electronic interactions from one metal center to the other. One can note that the wave separation is not as large as that determined for the 1,4-diethynylbenzene derivative ($|\Delta E_0| = 0.260$ V). Nevertheless it constitutes a significant interaction between the three iron centers, as evidenced by these observations. Despite the 1,3- or 1,3,5-substitution of the phenyl ring, which excludes a delocalization occurring through the participation of a quinoidal (quinonic) resonance structure, one can assume that there is a continuous overlap between the δ orbitals of the metal centers and the π orbitals of the polyethynylbenzene ligands.

Density Functional Calculations. The electronic structure of the title compounds were investigated with the aid of density functional molecular orbital calculations and compared to that of [{Fe(Cp*)(η^2-dppe)(C≡C−)}$_2$(1,4-C_6H_4)] (**4**) previously described.[28] The model compounds [{Fe(Cp)(PH_3)$_2$(C≡C−)}$_2$(1,3-C_6H_4)] (**2**-H), [{Fe(Cp)(PH_3)$_2$(C≡C−)}$_3$(1,3,5-C_6H_3)] (**3**-H) and [{Fe(Cp)(PH_3)$_2$(C≡C−)}$_2$(1,4-C_6H_4)] (**4**-H) were used in order to reduce computational effort. Calculations were made without symmetry constraints in order to allow the rotation of the Fe$Cp(PH_3)_2$ fragments around the central phenyl ring. However, only a partial optimization was performed, and a pseudosymmetry was kept for the metal−carbon core [Fe(C≡C−)]$_n$(C_6H_m) ($n = 2, 3$; $m = 4, 3$): C_{2v}, D_{3h}, and D_{2h} for **2**-H, **3**-H, and **4**-H, respectively.

Calculations carried out on models **2**-H, **3**-H, and **4**-H show a rather flat potential energy surface, indicating that the orientation of the Fe(Cp)(PH_3)$_2$ fragments relative to the plane of the phenyl ring has a negligible influence on the electronic and structural features of the metal−carbon core under investigation. Similar Fe−C and C−C distances are computed, and no noteworthy energy difference (less than 4.0 kJ/mol) is found for the different conformers of each model. We can conclude that the observed orientation of the Fe(Cp*)(η^2-dppe) units in **3** results from steric hindrance of the bulky dppe ligands and crystal lattice effects (vide supra). Therefore, the data presented here are for those models with the highest possible symmetry: C_{2v}, C_{3v}, and C_{2v} for **2**-H, **3**-H, and **4**-H, respectively. The optimized bond lengths for these models are given in Table 4.

Nearly identical Fe−C and C−C separations are found in **2**-H and **4**-H. The computed distances lead to Fe−Fe separations of 10.29 Å and 11.89 in **2**-H and **4**-H, respectively. It is noteworthy to mention that the total energies of models **2**-H and **4**-H are nearly similar ($\Delta E = 1.3$ kJ/mol, which is below the limit of accuracy of the method used). Indeed, the two complexes are isoenergetic. The Fe−C and C−C distances computed for **3**-H are few thousandths longer. They compare rather well with the bond lengths measured in the X-ray structure of 3. The largest deviation concerns the C−C distance of the benzene ring, computed to be 0.016 Å shorter than the experimental value. The computed

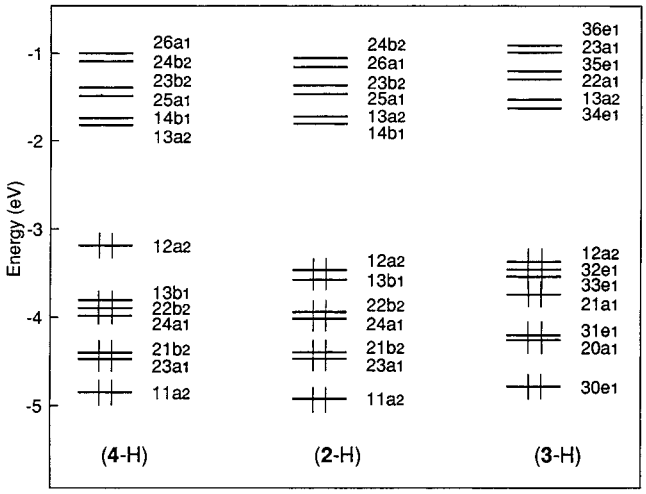

Figure 3. Frontier molecular orbitals for complexes **4**-H, **2**-H, and **3**-H of C_{2v}, C_{3v}, and C_{2v} symmetry, respectively.

Fe−Fe distance of 10.34 Å is very close to those measured experimentally (vide supra). The rather good comparison between the bond distances computed for **3**-H and the corresponding experimental bond lengths of **3** gives confidence in the computed bond distances in **2**-H and **4**-H, complexes used to model species **2** and **4** for which no X-ray data are available yet. This good agreement provides compelling evidence that the computational method used is reliable for predicting the bond lengths of organometallic systems.

The frontier molecular orbitals of the different optimized models **2**-H, **3**-H, and **4**-H are shown and compared in Figure 3. A rather large energy gap separates the occupied and vacant orbital sets in all models, as expected for 18-electron metal complexes. Though their electronic structures are comparable, we note that the HOMO−LUMO gap in **2**-H is larger by ca. 0.2 eV than that in **4**-H (1.66 vs 1.45 eV). This is due to the energy of the HOMO in **2**-H being lower than that of the HOMO in **4**-H. This is in agreement with the fact that the first oxidation potential of **2** is 0.09 V more positive than that of **4**. The HOMO−LUMO gap in **3**-H is 1.74 eV.

For a discussion of the chemical trends of the title compounds, particularly those concerning their electrochemical oxidation behavior, it is informative to look at the composition of the orbitals located in the HOMO region. The HOMO and HOMO-1 of the different models are sketched in Figures 4−6. A fragment analysis reveals that in **2**-H and **4**-H, these MOs (molecular orbitals) result from destabilizing four-electron−two-orbital interactions between the dπ orbitals of the Fe(Cp)(PH_3)$_2$ fragments[59] and out-of-plane π orbitals of the bis(ethynyl)benzene ligand. This differs from the result obtained by Lichtenberger et al. for Fe(Cp)(CO)$_2$(C≡CPh), the HOMO of which descends from an interaction of a dπ metal orbital with an in-plane π ligand orbital.[13] On the other hand, as in Fe(Cp)(CO)$_2$(C≡CPh), the HOMO in **3**-H derives from the interaction between metal dπ orbitals and an in-plane π/σ orbital of the tris(ethynyl)benzene ligand whereas the HOMO-1 results from mixing of the dπ orbitals and an out-of-plane π orbital, as in **2**-H and **4**-H. These MOs contain several nodes and are overall strongly localized on the Fe centers and the ethynyl groups and rather

(59) Schilling, B. E. R.; Hoffmann, R.; Llchtenberger, D. L. *J. Am. Chem. Soc.* **1979**, *101*, 585−591.

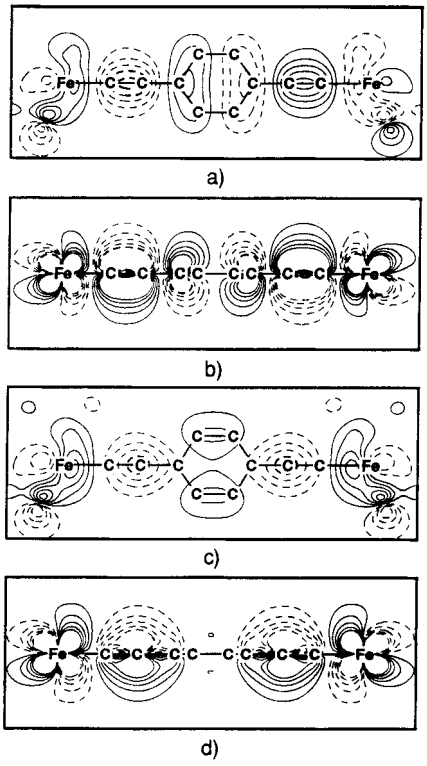

Figure 4. (a) Top view (1 Å above the plane of the phenyl ring) and (b) side view of the contour plot of the $12a_2$ π-HOMO of **4**-H and (c) top view (1 Å above the plane of the phenyl ring) and (d) side view of the contour plot of the $13b_1$ π-HOMO-1 of **4**-H. Contour values are ± 0.01, ± 0.02, ± 0.03, ± 0.04, and ± 0.05 [e/bohr^3]$^{1/2}$.

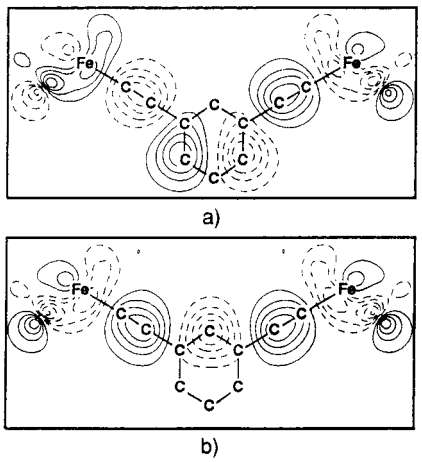

Figure 5. Contour plots (side view) of (a) the $12a_2$ π-HOMO and (b) the $13b_1$ π-HOMO-1 of **2**-H. See caption to Figure 3 for contour values.

poorly localized on the phenyl ring. Nevertheless, considering that the oxidation processes will affect these MOs in the mixed-valence compounds, it is likely to say that the bis- or tris(ethynyl)benzene ligand is a suitable connector for providing long-range electronic communication between two or three metal centers in a two-dimensional arrangement. DFT (density functional theory) calculations on the cationic species are in progress to confirm this statement.

The computed Mulliken atomic populations, which are given in Table 5, indicate that a slight electronic charge transfer takes place in the models **2**-H, **3**-H, and **4**-H. The carbon atoms of the benzene ring bearing the Fe(Cp)$(PH_3)_2$(ethynyl) groups are slightly positive, whereas those attached to hydrogen atoms are negative. Whatever the model, the β carbon atom of the ethynyl groups is more negatively charged than the α carbon atom, making the former more nucleophilic vis-à-vis electrophilic attack. This nucleophilic character is emphasized by the fact that the HOMO of each complex is importantly localized on the β carbon atoms (see Table 5).

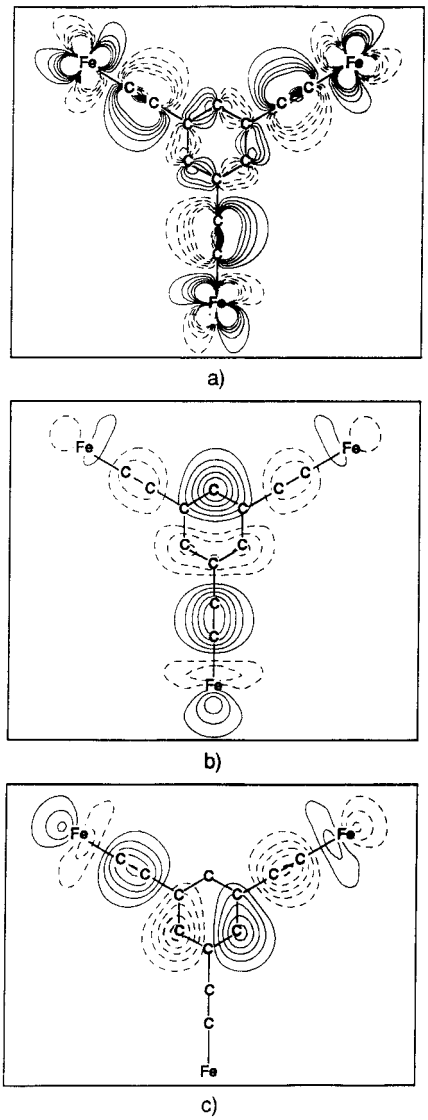

Figure 6. Contour plots (side view) of (a) the $12a_2$ π/σ-HOMO and (b and c) the 33e π-HOMO-1 of **3**-H. See caption to Figure 3 for contour values.

Table 5. Atomic Net Charges for Models 2-H, 3-H, and 4-H

	4-H	**2**-H	**3**-H
Fe	−0.24	−0.25	−0.29
C(α)	−0.07	−0.07	−0.05
C(β)	−0.19	−0.18	−0.17
C(1)[a]	+0.11	+0.12	+0.13
C(2)	−0.31	−0.35	−0.36
C(4)		−0.33	
C(5)	−0.31	−0.26	

[a] The carbon atoms of the phenyl ring are clockwise numbered, with C(1) attached to C(β).

Our experimental and theoretical results are complementary. Taken together, they shed some light on the nature of the interactions between the organometallic building blocks through the phenyl connector in the title compounds. The appropriate theories for the description of trinuclear mixed-valence compounds with more than one unpaired electron are not fully established yet,

and unambiguous experimental data are rare. The synthesis of the mixed-valence complexes $\mathbf{3}^{+}$ and $\mathbf{3}^{2+}$, which are accessible targets as shown from the CV measurements, will offer the stimulating opportunity of collecting spectroscopic data on such a class of compounds and comparing them with DFT calculations on these cationic species. This will be the focus of further efforts.

Experimental Section

General Data. Reagent grade tetrahydrofuran (THF), diethyl ether, and pentane were dried and distilled from sodium benzophenone ketyl prior to use. Pentamethylcyclopentadiene was prepared according to the published procedure,[60] and other chemicals were used as received. All of the manipulations were carried out under an argon atmosphere using Schlenk techniques or in a Jacomex 532 drybox filled with nitrogen. High-field NMR spectroscopy experiments were performed on a multinuclear Bruker 300 MHz instrument at 20 °C. Chemical shifts are given in parts per million (ppm) relative to tetramethylsilane (TMS) for the ^{1}H and ^{13}C NMR spectra and H_3PO_4 for ^{31}P NMR spectra. Cyclic voltamograms were recorded by using a PAR 263 instrument. Elemental analyses were performed at the Center for Microanalyses of the CNRS at Lyon-Solaise, France.

[{Fe(Cp*)(η^2-dppe)(C≡C)}$_2$-(1,3-C$_6$H$_4$)] (2). To a suspension of 0.75 g (2.8 mmol) of 1,3-bis(trimethylsilylethynyl)-benzene, 1.21 g (6.6 mmol) of KPF_6, and 0.38 g (6.6 mmol) of KF in 60 mL of MeOH/THF mixture (10:1) was added 4.16 g (6.6 mmol) of [Fe(η^5-C_5Me_5)(η^2-dppe)Cl]. The mixture was stirred under reflux (100 °C) for 12 h and the solvent was evaporated under vacuum. The solid residue was extracted with toluene, and the solution was evaporated to dryness. The solid was washed twice with 10 mL of pentane and dried in vacuo to give 2.9 g (2.2 mmol, 80%) of [{Fe(η^5-C_5Me_5)(η^2-dppe)-(C≡C)}$_2$(1,3-C_6H_4)] as an orange powder. Anal. Calcd for $C_{82}H_{82}Fe_2P_4$: C, 74.27; H, 6.26. Found: C, 74.41; H, 6.04 ($^1/_4$ CH_2Cl_2). FT-IR (Nujol, cm^{-1}): 2053 (ν C≡C). ^{1}H NMR (300 MHz, CD_2Cl_2): δ_H 7.85−7.20 (m, 24H, Ph), 2.69 and 2.06 (2m, 8H, CH_2), 1.26 (s, 30H, C_5Me_5). ^{31}P NMR (300 MHz, CD_2Cl_2): δ_P 89.37. ^{13}C NMR{^{1}H} (75 MHz, CD_2Cl_2): δ_C 134.9−127.0 (m, Ph), 88.6 (s, C_5Me_5), 30.1 (m, CH_2), 10.2 (s, C_5Me_5). Mössbauer (mm/s vs Fe, 80 K): IS 0.200, QS 2.000. UV (CH_2Cl_2): λ_{max} (ϵ, 103 dm^3·mol^{-1}·cm^{-1}) 254 (28.0), 349 (15.0), 688 (0.2).

[{Fe(Cp*)(η^2-dppe)(C≡C)}$_3$-(1,3,5-C$_6$H$_3$)]. To a suspension of 0.5 g (1.36 mmol) of 1,3,5-tris(trimethylsilylethynyl)-benzene, 0.80 g (3.2 equiv) of KPF_6, and 0.25 g (3.2 equiv) of KF in 60 mL of MeOH/THF mixture (10:1) was added 3.00 g (3.2 equiv) of [Fe(Cp*)(η^2-dppe)Cl]. The mixture was stirred under reflux for 48 h. To complete the reaction, 0.32 g (1.3 equiv) of KPF_6, 0.10 g (1.3 equiv) of KF, and 1.1 g (1.3 equiv) of [Fe(η^5-C_5Me_5)(η^2-dppe)Cl] were then added, and reflux continued for 12 h more. The solvent was evaporated under vacuum, and the residue was extracted with toluene. The solid was washed twice with 10 mL of pentane and dried in vacuo to give 2.1 g (1.10 mmol) of [{Fe(η^5-C_5Me_5)(η^2-dppe)(C≡C)}$_3$-{1,3,5-C_6H_3}] as an orange powder (80% yield). Anal. Calcd for $C_{120}H_{120}Fe_3P_6$: C, 75.24; H, 6.31. Found: C, 74.9; H, 6.29 ($^1/_8$ CH_2Cl_2). FT-IR (Nujol, cm^{-1}): 2051 (ν C≡C). ^{1}H NMR (300 MHz, CD_2Cl_2): δ_H 7.86−7.18 (m, 63H, Ph) 2.75 and 1.95 (2m, 12H, CH_2), 1.39 (s, 45H, C_5Me_5). ^{31}P NMR: δ_P 101.3. ^{13}C NMR{^{1}H} (75 MHz, CD_2Cl_2): δ_C 138.3−127.5 (m, Ph), 88.1 (s, C_5Me_5), 30.1 (m, CH2); 10.2 (s, C_5Me_5). Mössbauer (mm/s vs Fe, 80 K): IS 0.257, QS 1.992. UV (CH_2Cl_2): λ_{max} (ϵ, 103 dm^3·mol^{-1}·cm^{-1}) 283 (53.4), 351 (35.0), 712 (0.7).

X-ray Crystallography for 3. Crystals suitable for single X-ray diffraction studies were obtained from dichloromethane−pentane at 20 °C. The data were measured on a CAD-4 Enraf-Nonius automated diffractometer. All of the calculations were performed on a Digital MicroVax 3100 computer with the MOLEN package.[61] Crystal data collection and refinement parameters are collected in Table 1. The rather low data to parameter ratio (6.17) is the result of a compromise between a not too low cut-off value and a very large number of variables. After Lorentz polarization corrections, the structure was solved by direct methods, which located many of the non-hydrogen atoms of the structure. The remaining non-hydrogen atoms were located after successive scale factor refinements and Fourier differences. After isotropic (R = 0.81) and anisotropic refinements (R = 0.069), many hygrogen atoms were found with a Fourier difference and the others were set in theoretical positions. The whole structure was refined on F by the full-matrix least-squares techniques (use of F magnitude; x, y, z, β_{ij} for Fe, P, and C atoms, x, y, z, B_{iso} for the methyl groups of the Cp*; 1124 variables and 6922 observations).

Density Functional Calculations. Density functional calculations[62] were carried out on models **2**-H, **3**-H, and **4**-H using the Amsterdam Density Functional (ADF) program[63] developed by Baerends and co-workers[64−67] using nonlocal exchange and correlation corrections.[68−70] The geometry optimization procedure was based on the method developed by Versluis and Ziegler.[71] The atom electronic configurations were described by a double-ζ Slater-type orbital basis set for H 1s, C 2s and 2p, and P 3s and 3p, augmented with a 3d single-ζ polarization function for the carbon atoms of the bis- or tris(ethynyl)benzene ligand. A triple-ζ STO basis set was used for Fe 3d and 4s, augmented with a single-ζ 4p polarization function. A frozen-core approximation was used to treat the core electrons of C, P, and Fe. For convenience, calculations on **3**-H were made using a C_{3v} symmetry instead of a C_{3h} symmetry.

Acknowledgment. We are grateful to Dr. S. Sinbandhit (C. R. M. P. O., Rennes) for NMR assistance. M.J.C. and J.-F.H. thank Pr. Baerends and Dr. te Velde (Vrije Universiteit, Amsterdam) for introducing them to the ADF program. Exchanges between the groups of Amsterdam, Oeiras, and Rennes have been made possible through an European Human Capital and Mobility Network (ERBCHRXCT-930156). J.-F.H. thanks the Centre de Ressources Informatiques (CRI) of Rennes and the Institut de Développement et de Ressources en Informatique Scientifique (IDRIS-CNRS) of Orsay (Project 950649) for computing facilities. We are also indebted to the Laboratoires Standa (Caen, France) and to the Région Bretagne for financial support to T.W. and G.F., respectively.

Supporting Information Available: Complete tables of bond lengths, bond angles, atomic coordinates, and general temperature factor expressions, ORTEP diagram, and ^{31}P NMR spectrum of **3** (38 pages). Ordering information is given on any current masthead page.

OM961102U

(60) Mays, M. J.; Sears, P. L. *J. Chem. Soc., Dalton Trans.* **1973**, 1873−1875.

(61) Fair, C. K. *MOLEN. An Interactive System for Crystal Structure Analysis*; Enraf-Nonius: Delft, The Netherlands, 1990.

(62) Parr, R. G.; Wang, W. *Density-Functional Theory of Atoms and Molecules*; Oxford University: New York, 1989.

(63) *Amsterdam Density Functional (ADF) Program*, release 2.0.1; Vrije Universiteit: Amsterdam, The Netherlands, 1996.

(64) Baerends, E. J.; Ellis, D. E.; Ros, P. *Chem. Phys.* **1973**, *2*, 41−51.

(65) Baerends, E. J.; Ros, P. *Int. J. Quantum Chem.* **1978**, *S12*, 169−190.

(66) Boerrigter, P. M.; Te Velde, G.; Baerends, E. *J. Int. J. Quantum Chem.* **1988**, *33*, 87−113.

(67) Te Velde, G.; Baerends, E. J. *J. Comput. Phys.* **1992**, *99*, 84−98.

(68) Becke, A. D. *Phys. Rev.* **1988**, *A38*, 3098−3100.

(69) Vosko, S. D.; Wilk, L.; Nusair, M. *Can. J. Chem.* **1990**, *58*, 1200−1207.

(70) Perdew, J. P. *Phys. Rev.* **1986**, *B34*, 7406.

(71) Verluis, L.; Ziegler, T. *J. Chem. Phys.* **1988**, *88*, 322−328.